

Synthesis and Structure of Lewis Base Adducts of $[\text{Et}_4\text{N}]_2[\text{Tl}_2\text{Fe}_4(\text{CO})_{16}]$

Juanita M. Cassidy and Kenton H. Whitmire*

Received August 8, 1988

The thallium-iron compound $[\text{Et}_4\text{N}]_2[\text{Tl}_2\text{Fe}_4(\text{CO})_{16}]$, believed to exist as the monomer, $[\text{Et}_4\text{N}][\text{TlFe}_2(\text{CO})_8]$, in solution, reacts with Lewis bases to form the adducts $[\text{Et}_4\text{N}](\text{L})\text{TlFe}_2(\text{CO})_8$ (L = 2,2'-bipyridine (bpy), 1,10-phenanthroline (phen), *N,N,N',N'*-tetramethylethylenediamine (TMEDA), diethylenetriamine (dien), ethylenediamine (en)), with a Lewis base to thallium ratio of 1:1. In each case the thallium exhibits a highly distorted tetrahedral environment, being bonded to two $\text{Fe}(\text{CO})_4$ groups and to two nitrogens of the Lewis base ligand. The $\text{Fe}(\text{CO})_4$ groups are trigonal bipyramidal with Tl occupying an axial position. The crystal data of several of these adducts were collected on a Rigaku AFC5S diffractometer using Mo $K\alpha$ radiation. $[\text{Et}_4\text{N}](\text{bpy})\text{TlFe}_2(\text{CO})_8$ crystallizes in the monoclinic space group $C2/c$ with $a = 12.516$ (5) Å, $b = 18.430$ (5) Å, $c = 13.11$ (1) Å, $\beta = 94.24$ (4)°, $V = 3015$ (3) Å³, and $Z = 4$. The phenanthroline adduct is isomorphous with the bipyridine adduct: monoclinic space group $C2/c$ with $a = 12.197$ (6) Å, $b = 19.284$ (8) Å, $c = 13.243$ (2) Å, $\beta = 92.54$ (3)°, $V = 3112$ (4) Å³, and $Z = 4$. Crystals of $[\text{Et}_4\text{N}](\text{TMEDA})\text{TlFe}_2(\text{CO})_8$ are orthorhombic, space group $Pbca$, with $a = 17.541$ (3) Å, $b = 17.530$ (3) Å, $c = 19.683$ (4) Å, $V = 6052$ (3) Å³, and $Z = 8$. $[\text{Et}_4\text{N}](\text{dien})\text{TlFe}_2(\text{CO})_8$ forms crystals with centrosymmetric space group $P2_1/n$ with $a = 15.667$ (6) Å, $b = 7.770$ (1) Å, $c = 23.585$ (2) Å, $\beta = 97.92$ (2)°, $V = 2844$ (1) Å³, and $Z = 4$. The ethylenediamine adduct, $[\text{Et}_4\text{N}](\text{en})\text{TlFe}_2(\text{CO})_8$, was also produced and was characterized by spectroscopic data and elemental analysis. Steric and electronic factors affecting the geometries of these adducts are discussed.

Introduction

Recently several main-group/transition-metal thallium-iron carbonyls have been reported, including $[\text{Et}_4\text{N}]_2[\text{Tl}_2\text{Fe}_4(\text{CO})_{16}]$,^{1a} $[\text{Et}_4\text{N}]_4[\text{Tl}_4\text{Fe}_8(\text{CO})_{30}]$,^{1a} and $[\text{Et}_4\text{N}]_6[\text{Tl}_6\text{Fe}_{10}(\text{CO})_{36}]$.^{1a,2} The terminal thallium-iron bond distances are short when compared to the other thallium-iron bonds existing in these same compounds, and the possible presence of multiple bonding has been suggested,¹ but since no Tl-Fe compounds had previously been structurally characterized, no bond data existed for comparison. Thus, a Tl-Fe compound was sought to establish a Tl-Fe single-bond distance. Furthermore, in solution, the compound $[\text{Et}_4\text{N}]_2[\text{Tl}_2\text{Fe}_4(\text{CO})_{16}]$ is believed to exist as the electron-deficient monomer $[\text{Et}_4\text{N}][\text{TlFe}_2(\text{CO})_8]$ ($[\text{Et}_4\text{N}][\text{I}]$),^{1a} which might be expected to form electron-precise Lewis base adducts. The acidity of the Tl center in $[\text{Et}_4\text{N}][\text{I}]$ was confirmed by the synthesis of several Lewis base adducts— $[\text{Et}_4\text{N}](\text{bpy})\text{TlFe}_2(\text{CO})_8$ (bpy = 2,2'-bipyridine; $[\text{Et}_4\text{N}][\text{Ia}]$), $[\text{Et}_4\text{N}](\text{phen})\text{TlFe}_2(\text{CO})_8$ (phen = 1,10-phenanthroline; $[\text{Et}_4\text{N}][\text{Ib}]$), $[\text{Et}_4\text{N}](\text{TMEDA})\text{TlFe}_2(\text{CO})_8$ (TMEDA = *N,N,N',N'*-tetramethylethylenediamine; $[\text{Et}_4\text{N}][\text{Ic}]$), and $[\text{Et}_4\text{N}](\text{dien})\text{TlFe}_2(\text{CO})_8$ (dien = diethylenetriamine; $[\text{Et}_4\text{N}][\text{Id}]$). The solid-state structural characterizations of these compounds are reported herein. The ethylenediamine adduct was also produced and was formulated as $[\text{Et}_4\text{N}](\text{en})\text{TlFe}_2(\text{CO})_8$ ($[\text{Et}_4\text{N}][\text{Ie}]$) on the basis of spectroscopic data and elemental analyses.

Experimental Section

The thallium-iron adducts described are moderately air sensitive in solution, and the reactions were performed under an oxygen-free nitrogen atmosphere by using standard Schlenk techniques. The organic solvents used were dried and distilled under nitrogen. The starting compound $[\text{Et}_4\text{N}]_2[\text{Tl}_2\text{Fe}_4(\text{CO})_{16}]$ was synthesized according to the previously reported method.^{1a} Ethylenediamine was dried by heating over KOH for several hours followed by distillation, and 1,10-phenanthroline was purified by recrystallization. All other reagents were used as received from commercial sources. Spectra were obtained by using a PE 1430 infrared spectrophotometer and a JEOL FX90Q NMR spectrometer. Elemental analyses were performed by Galbraith Analytical Laboratories (Knoxville, TN).

$[\text{Et}_4\text{N}](\text{bpy})\text{TlFe}_2(\text{CO})_8$ ($[\text{Et}_4\text{N}][\text{Ia}]$). To a solution of 150 mg (0.112 mmol) of $[\text{Et}_4\text{N}]_2[\text{Tl}_2\text{Fe}_4(\text{CO})_{16}]$ in 10 mL of methanol was added an excess (40 mg, 0.3 mmol) of 2,2'-bipyridine. The solution color changed gradually from brown-orange to red-orange. The solution was concentrated under vacuum and cooled to form orange-red crystals: yield

85.3%; mp 138–142 °C. IR (MeOH, cm^{-1}): 2008 (sh), 2000 (sh), 1980 (s), 1910 (s). IR (Nujol mull, cm^{-1}): 2000 (m), 1963 (s), 1913 (s), 1860 (s, br). Anal. Calcd: Tl, 24.73; N, 5.08. Found: Tl, 24.29; N, 4.96.

$[\text{Et}_4\text{N}](\text{phen})\text{TlFe}_2(\text{CO})_8$ ($[\text{Et}_4\text{N}][\text{Ib}]$). To a solution of 100 mg (0.075 mmol) of $[\text{Et}_4\text{N}]_2[\text{Tl}_2\text{Fe}_4(\text{CO})_{16}]$ in 10 mL of methylene chloride was added 27 mg (0.15 mmol) of 1,10-phenanthroline. The solution color changed gradually from brown-orange to red-orange. The solution was concentrated and cooled to yield red-orange crystals: yield 59.4%; mp dec >190 °C. IR (CH_2Cl_2 , cm^{-1}): 2000 (m), 1985 (s), 1965 (s), 1889 (s, br). IR (Nujol mull, cm^{-1}): 2000 (m), 1964 (s), 1911 (s), 1860 (s, br). Anal. Calcd: Tl, 24.03; N, 4.94. Found: Tl, 23.03; N, 4.88.

$[\text{Et}_4\text{N}](\text{en})\text{TlFe}_2(\text{CO})_8$ ($[\text{Et}_4\text{N}][\text{Ie}]$). This compound was prepared by adding excess (1 mL) ethylenediamine to a solution of 150 mg (0.112 mmol) of $[\text{Et}_4\text{N}]_2[\text{Tl}_2\text{Fe}_4(\text{CO})_{16}]$ in 10 mL of methanol. The solution color slowly changed from brown-orange to orange. The solution was concentrated and cooled to yield hexagonal plate crystals that varied in color from yellow to red depending on the thickness: yield 86.8%; mp 126–130 °C. IR (CH_2Cl_2 , cm^{-1}): 2000 (m), 1984 (s), 1964 (s), 1889 (s, br). IR (Nujol mull, cm^{-1}): 1990 (m), 1971 (s), 1955 (s), 1855 (s, br). Anal. Calcd: Tl, 27.99; N, 5.75. Found: Tl, 27.99; N, 5.56.

$[\text{Et}_4\text{N}](\text{TMEDA})\text{TlFe}_2(\text{CO})_8$ ($[\text{Et}_4\text{N}][\text{Ic}]$). To a brown-orange solution of 150 mg (0.112 mmol) of $[\text{Et}_4\text{N}]_2[\text{Tl}_2\text{Fe}_4(\text{CO})_{16}]$ in 10 mL of methanol was added excess (0.5 mL) *N,N,N',N'*-tetramethylethylenediamine. The solution gradually became dark red. Anhydrous diethyl ether was added to the concentrated solution, and dark red crystals formed upon cooling: yield 69.9%; mp 108–112 °C. IR (MeOH, cm^{-1}): 1980 (s), 1910 (s). IR (Nujol mull, cm^{-1}): 1994 (s), 1969 (s, sh), 1957 (s), 1907 (s), 1868 (s, br). Anal. Calcd: Tl, 25.99; N, 5.35. Found: Tl, 25.91; N, 4.62.

$[\text{Et}_4\text{N}](\text{dien})\text{TlFe}_2(\text{CO})_8$ ($[\text{Et}_4\text{N}][\text{Id}]$). Diethylenetriamine (0.5 mL) was added directly to 150 mg (0.112 mmol) of $[\text{Et}_4\text{N}]_2[\text{Tl}_2\text{Fe}_4(\text{CO})_{16}]$. The $[\text{Et}_4\text{N}]_2[\text{Tl}_2\text{Fe}_4(\text{CO})_{16}]$ slowly dissolved in the diethylenetriamine to give an orange red oil. The oil was washed once with several volumes of anhydrous diethyl ether. Then diethyl ether was layered on top of the oil, and the solution was cooled. The resulting orange to red needlelike crystals were washed with hexane several times: yield 78.6%; mp 105–133 °C. IR (Acetone, cm^{-1}): 1997 (m), 1982 (s), 1964 (s), 1888 (s, br). IR (Nujol mull, cm^{-1}): 1988 (m), 1951 (s), 1810 (s, br).

X-ray Analyses of $[\text{Et}_4\text{N}][\text{Ia}]$, $[\text{Et}_4\text{N}][\text{Ib}]$, $[\text{Et}_4\text{N}][\text{Ic}]$, and $[\text{Et}_4\text{N}][\text{Id}]$. X-ray-quality crystals of the adducts were obtained by the following methods: $[\text{Et}_4\text{N}][\text{Ia}]$, by concentrating a MeOH solution of 0.15 g (0.11 mmol) of $[\text{Et}_4\text{N}]_2[\text{Tl}_2\text{Fe}_4(\text{CO})_{16}]$ and excess 2,2'-bipyridine; $[\text{Et}_4\text{N}][\text{Ib}]$, by cooling an acetone (10 mL)/benzene (1 mL) solution containing 0.100 g (0.075 mmol) of $[\text{Et}_4\text{N}]_2[\text{Tl}_2\text{Fe}_4(\text{CO})_{16}]$ and 0.027 g (0.15 mmol) of 1,10-phenanthroline and recrystallizing from CH_2Cl_2 /diethyl ether; $[\text{Et}_4\text{N}][\text{Ic}]$, by reaction of 0.5 mL (excess) of *N,N,N',N'*-tetramethylethylenediamine with 0.15 g (0.11 mmol) of $[\text{Et}_4\text{N}]_2[\text{Tl}_2\text{Fe}_4(\text{CO})_{16}]$ in 9 mL of MeOH, followed by filtration, addition of diethyl ether and cooling; $[\text{Et}_4\text{N}][\text{Id}]$, by addition of 1 mL of diethylenetriamine to a solution of 125 mg (0.094 mmol) of $[\text{Et}_4\text{N}]_2[\text{Tl}_2\text{Fe}_4(\text{CO})_{16}]$ in 10 mL of methanol, followed by several washings with anhydrous diethyl ether. Crystal dimensions were $0.2 \times 0.3 \times 0.3$ mm³ for $[\text{Et}_4\text{N}][\text{Ia}]$, $0.1 \times 0.1 \times 0.2$ mm³ for $[\text{Et}_4\text{N}][\text{Ib}]$, and $0.2 \times 0.3 \times 0.5$ mm³ for $[\text{Et}_4\text{N}][\text{Id}]$. The crystals were mounted on glass fibers by using epoxy cement. All pro-

- (1) (a) Whitmire, K. H.; Cassidy, J. M.; Rheingold, A. L.; Ryan, R. R. *Inorg. Chem.* 1987, 27, 1347. (b) For a review on main-group/transition-metal multiple bonding, see: Herrmann, W. A. *Angew. Chem., Int. Ed. Engl.* 1986, 25, 56.
(2) Whitmire, K. H.; Ryan, R. R.; Wasserman, H. J.; Albright, T. A.; Kang, S.-K. *J. Am. Chem. Soc.* 1986, 108, 6831.

Table I. Crystallographic Data for [Et₄N][bpy]TiFe₂(CO)₈, [Et₄N][phen]TiFe₂(CO)₈, [Et₄N][TMEDA]TiFe₂(CO)₈, and [Et₄N][dien]TiFe₂(CO)₈

compd	[Et ₄ N][Ia]	[Et ₄ N][Ib]	[Et ₄ N][Ic]	[Et ₄ N][Id]
empirical formula	C ₂₆ H ₂₈ Fe ₂ N ₃ O ₈ Tl	C ₂₈ H ₂₈ Fe ₂ N ₃ O ₈ Tl	C ₂₂ H ₃₆ Fe ₂ N ₃ O ₈ Tl	C ₂₀ H ₃₃ Fe ₂ N ₄ O ₈ Tl
fw	826.59	850.61	786.61	773.57
lattice params				
<i>a</i> , Å	12.516 (5)	12.197 (6)	17.541 (3)	15.667 (6)
<i>b</i> , Å	18.430 (5)	19.284 (8)	17.530 (3)	7.770 (1)
<i>c</i> , Å	13.11 (1)	13.243 (2)	19.683 (4)	23.585 (2)
β, deg	94.24 (4)	92.54 (3)		97.92 (2)
<i>V</i> , Å ³	3015 (3)	3112 (4)	6052 (3)	2844 (1)
space group	C2/c (No. 15)	C2/c (No. 15)	<i>Pbca</i> (No. 61)	<i>P2₁/n</i> (No. 14)
<i>Z</i>	4	4	8	4
<i>D</i> _{calcd} , g cm ⁻³	1.82	1.82	1.73	1.81
μ(Mo Kα), cm ⁻¹	63.95	62.00	63.66	67.74
radiation			Mo Kα (λ = 0.71069 Å)	
temp			23 °C	
transmission coeff	0.4633–1.0000	0.6372–1.0000	0.5474–1.0000	0.6063–1.0000
<i>R</i> ; <i>R</i> _w	0.048; 0.059	0.049; 0.058	0.059; 0.057	0.053; 0.066

Table II. Positional Parameters and *B*(eq) for [Et₄N][Ia]

atom	<i>x</i>	<i>y</i>	<i>z</i>	<i>B</i> (eq), Å ²
Tl	0	0.23769 (3)	1/4	3.34 (3)
Fe1	0.1920 (1)	0.27035 (9)	0.3169 (1)	3.60 (7)
O1	0.230 (1)	0.3090 (7)	0.1079 (8)	7.8 (6)
O2	0.0965 (9)	0.3812 (6)	0.4397 (8)	7.5 (6)
O3	0.2062 (7)	0.1188 (5)	0.3842 (8)	6.1 (5)
O4	0.4088 (8)	0.3054 (6)	0.392 (1)	7.9 (6)
N1	0.0453 (7)	0.1167 (5)	0.1589 (7)	4.0 (5)
N2	1/2	0.0716 (9)	1/4	4.9 (7)
C1A	0.0315 (9)	0.0536 (6)	0.2027 (9)	3.8 (5)
C1C	0.133 (1)	-0.006 (1)	0.076 (1)	6.6 (8)
C1E	0.100 (1)	0.1199 (7)	0.075 (1)	4.5 (6)
C1	0.210 (1)	0.2932 (7)	0.190 (1)	4.5 (6)
C1B	0.072 (1)	-0.0115 (7)	0.165 (1)	5.9 (7)
C1D	0.143 (1)	0.0593 (9)	0.031 (1)	5.8 (8)
C2	0.131 (1)	0.3368 (8)	0.391 (1)	4.6 (6)
C3	0.198 (1)	0.1777 (7)	0.357 (1)	4.3 (6)
C4	0.322 (1)	0.2912 (7)	0.362 (1)	5.1 (6)
C11	0.509 (2)	0.122 (1)	0.157 (1)	9 (1)
C12	0.409 (1)	0.164 (1)	0.126 (2)	12 (1)
C21	0.402 (2)	0.030 (2)	0.241 (2)	15 (2)
C22	0.385 (2)	-0.020 (1)	0.335 (2)	11 (1)

Table III. Positional Parameters and *B*(eq) for [Et₄N][Ib]

atom	<i>x</i>	<i>y</i>	<i>z</i>	<i>B</i> (eq), Å ²
Tl	0	0.24478 (5)	1/4	3.73 (4)
Fe1	-0.1951 (2)	0.2717 (1)	0.1788 (2)	4.3 (1)
O1	-0.243 (1)	0.3041 (8)	0.385 (1)	9 (1)
O2	-0.102 (1)	0.3847 (7)	0.065 (1)	8.2 (9)
O3	-0.196 (1)	0.1293 (6)	0.108 (1)	6.8 (7)
O4	-0.417 (1)	0.2888 (7)	0.097 (1)	8.2 (9)
N1	-0.051 (1)	0.1308 (6)	0.338 (1)	4.3 (6)
N2	1/2	0.066 (1)	1/4	6 (1)
C1	-0.223 (1)	0.292 (1)	0.301 (1)	6 (1)
C2	-0.136 (2)	0.338 (1)	0.110 (1)	6 (1)
C3	-0.191 (1)	0.1857 (8)	0.135 (1)	4.6 (8)
C4	-0.326 (2)	0.283 (1)	0.128 (1)	7 (1)
C11	-0.105 (2)	0.132 (1)	0.424 (1)	7 (1)
C12	-0.143 (2)	0.070 (1)	0.473 (2)	8 (1)
C13	-0.119 (2)	0.008 (1)	0.433 (2)	10 (2)
C14	-0.058 (2)	0.0056 (9)	0.344 (2)	8 (1)
C15	-0.030 (1)	0.0698 (7)	0.295 (1)	4.8 (8)
C16	-0.031 (4)	-0.057 (1)	0.292 (3)	13 (3)
C31	0.594 (3)	0.027 (2)	0.251 (4)	19 (3)
C32	0.627 (3)	-0.016 (1)	0.173 (2)	13 (2)
C41	0.509 (5)	0.109 (2)	0.170 (3)	22 (4)
C42	0.410 (2)	0.153 (2)	0.123 (3)	13 (2)

grams used to solve the structures are part of the Molecular Structure Corp. data reduction and refinement programs (TEXSAN, version 2.0). Heavy-atom positions for [Et₄N][Ia], [Et₄N][Ib], and [Et₄N][Id] were located by using the program MITHRIL,³ SHELXS⁴ was used for [Et₄N][Ic].

(3) Gilmore, G. J. "MITHRIL: A Computer Program for the Automatic Solution of Crystal Structures from X-ray Data", University of Glasgow, Scotland, 1983.

Table IV. Positional Parameters and *B*(eq) for [Et₄N][Ic]

atom	<i>x</i>	<i>y</i>	<i>z</i>	<i>B</i> (eq), Å ²
Tl1	0.11055 (5)	0.81430 (5)	0.08034 (5)	4.44 (4)
Fe1	0.2421 (2)	0.8663 (2)	0.0392 (2)	5.2 (2)
Fe2	0.0260 (2)	0.8264 (2)	0.1891 (2)	5.3 (2)
O11	0.168 (1)	1.010 (1)	0.040 (1)	11 (2)
O12	0.238 (1)	0.780 (1)	-0.086 (1)	10 (1)
O13	0.294 (1)	0.789 (1)	0.161 (1)	12 (2)
O14	0.387 (1)	0.932 (1)	0.012 (1)	10 (1)
O21	0.017 (1)	0.982 (1)	0.143 (1)	9 (1)
O22	0.149 (1)	0.752 (1)	0.256 (1)	11 (2)
O23	-0.095 (1)	0.724 (1)	0.145 (1)	10 (1)
O24	-0.045 (1)	0.867 (1)	0.314 (1)	11 (2)
C11	0.195 (1)	0.949 (1)	0.039 (2)	7 (2)
C12	0.240 (2)	0.815 (1)	-0.033 (2)	7 (2)
C13	0.271 (1)	0.820 (2)	0.109 (2)	7 (2)
C14	0.329 (2)	0.906 (1)	0.025 (1)	6 (2)
C21	0.025 (2)	0.919 (2)	0.161 (1)	8 (2)
C22	0.103 (1)	0.785 (1)	0.227 (1)	6 (1)
C23	-0.043 (1)	0.764 (2)	0.161 (1)	7 (2)
C24	-0.017 (2)	0.848 (2)	0.263 (1)	7 (2)
N1	0.016 (1)	0.811 (1)	-0.025 (1)	7 (1)
N2	0.101 (1)	0.671 (1)	0.038 (1)	6 (1)
C1A	0.051 (2)	0.846 (2)	-0.088 (1)	10 (2)
C1B	-0.058 (1)	0.853 (2)	-0.004 (1)	9 (2)
C2A	0.180 (1)	0.639 (1)	0.031 (2)	9 (2)
C2B	0.054 (2)	0.623 (1)	0.084 (1)	9 (2)
C3A	0.065 (2)	0.673 (2)	-0.027 (2)	8 (2)
C3B	-0.002 (2)	0.725 (2)	-0.033 (1)	9 (2)
N3	0.733 (1)	0.011 (1)	0.212 (1)	7 (1)
C*11	0.681 (2)	0.038 (2)	0.154 (2)	12 (1)
C*12	0.600 (2)	-0.004 (2)	0.162 (1)	9.9 (8)
C*21	0.701 (2)	0.027 (2)	0.285 (2)	15 (1)
C*22	0.675 (2)	0.116 (2)	0.282 (2)	11 (1)
C*31	0.803 (2)	0.063 (2)	0.198 (2)	12 (1)
C*32	0.870 (2)	0.047 (2)	0.252 (2)	13 (1)
C*41	0.748 (2)	-0.075 (2)	0.213 (2)	12 (1)
C*42	0.789 (2)	-0.093 (2)	0.141 (2)	12 (1)

Subsequent refinements were performed by using full-matrix least-squares refinement. Corrections for non-hydrogen scattering factors and anomalous dispersion were made for all of the compounds.⁵ [Et₄N][Ib] was corrected for absorption (*ψ* scans), while both decay and absorption (*ψ* scans) corrections were applied for [Et₄N][Ia], [Et₄N][Ic], and [Et₄N][Id]. For [Et₄N][Ia] and [Et₄N][Ib], all atoms were refined anisotropically, and for [Et₄N][Ic] and [Et₄N][Id], all atoms except the carbons on the [Et₄N]⁺ cation were refined anisotropically. Hydrogen-bond parameters were calculated for the diethylenetriamine adduct, [Et₄N][Id], only. Crystallographic data for [Et₄N][Ia], [Et₄N][Ib], [Et₄N][Ic], and [Et₄N][Id] are listed in Table I. Cell constants for [Et₄N][Ic] indicate a tetragonal cell. However, measurement of re-

(4) Sheldrick, G. M. "SHELXS86: A Program for Crystal Structure Determination", University of Göttingen, Göttingen, Federal Republic of Germany.

(5) Cromer, D. T.; Waber, J. T. *International Tables for X-ray Crystallography*; Kynoch Press: Birmingham, England, 1974; Vol IV, pp 71 and 148.

Table V. Positional Parameters for $[\text{Et}_4\text{N}][\text{Id}]$

atom	x	y	z	$B(\text{eq}), \text{\AA}^2$
Tl1	0.51626 (4)	0.54202 (7)	0.24919 (2)	4.21 (3)
Fe1	0.4962 (1)	0.4449 (3)	0.14248 (8)	4.3 (1)
Fe2	0.5344 (1)	0.4302 (3)	0.35476 (8)	4.3 (1)
O11	0.3282 (9)	0.320 (2)	0.1645 (6)	8.6 (8)
O12	0.6585 (8)	0.265 (2)	0.1735 (5)	7.6 (7)
O13	0.518 (1)	0.797 (2)	0.1061 (5)	8.7 (8)
O14	0.4664 (8)	0.309 (2)	0.0282 (5)	9.2 (9)
O21	0.502 (1)	0.783 (2)	0.3901 (5)	8.6 (8)
O22	0.7060 (9)	0.334 (2)	0.3342 (6)	10 (1)
O23	0.382 (1)	0.228 (2)	0.3145 (6)	10 (1)
O24	0.556 (1)	0.281 (2)	0.4693 (6)	12 (1)
C11	0.396 (1)	0.367 (2)	0.1587 (7)	6 (1)
C12	0.594 (1)	0.332 (2)	0.1646 (6)	5.1 (8)
C13	0.510 (1)	0.656 (2)	0.1217 (7)	6 (1)
C14	0.477 (1)	0.360 (2)	0.0729 (6)	5.6 (8)
C21	0.515 (1)	0.639 (3)	0.3744 (7)	6 (1)
C22	0.638 (1)	0.377 (2)	0.3401 (6)	5.6 (8)
C23	0.443 (1)	0.307 (2)	0.3284 (7)	7 (1)
C24	0.546 (1)	0.338 (2)	0.4232 (7)	5.9 (9)
N1	0.6567 (7)	0.725 (2)	0.2522 (5)	5.5 (7)
N2	0.4863 (8)	0.865 (2)	0.2533 (5)	4.9 (6)
N3	0.335 (1)	0.671 (3)	0.249 (1)	11 (1)
C1	0.641 (1)	0.901 (3)	0.2702 (9)	8 (1)
C2	0.558 (1)	0.969 (2)	0.2429 (9)	7 (1)
C3	0.404 (1)	0.908 (3)	0.223 (1)	8 (1)
C4	0.331 (2)	0.836 (4)	0.251 (2)	14 (2)
N4	0.2539 (8)	0.243 (2)	0.4909 (5)	5.2 (7)
C1A	0.284 (2)	0.165 (5)	0.544 (2)	19 (1)
C2A	0.245 (2)	0.129 (5)	0.434 (1)	17 (1)
C3A	0.330 (2)	0.352 (6)	0.487 (2)	20 (1)
C4A	0.166 (2)	0.302 (5)	0.483 (1)	17 (1)
C1B	0.223 (1)	-0.010 (3)	0.553 (1)	9.3 (6)
C2B	0.346 (1)	0.036 (3)	0.4399 (9)	8.7 (5)
C3B	0.292 (2)	0.489 (3)	0.429 (1)	10.7 (7)
C4B	0.164 (1)	0.451 (3)	0.540 (1)	9.7 (6)
H1	0.7010	0.6747	0.2786	6.6
H2	0.6740	0.7271	0.2152	6.6
H3	0.4807	0.8854	0.2923	5.9
H4	0.3002	0.6320	0.2154	12.9
H5	0.3130	0.6265	0.2818	12.9
H6	0.6420	0.9030	0.3106	9.5
H7	0.6858	0.9734	0.2602	9.5
H8	0.5589	0.9744	0.2029	8.9
H9	0.5503	1.0807	0.2575	8.9
H10	0.3984	1.0300	0.2217	10.0
H11	0.3998	0.8643	0.1851	10.0
H12	0.2781	0.8742	0.2306	17.2
H13	0.3367	0.8736	0.2893	17.2

Table VI. Selected Bond Distances and Angles for $[\text{Et}_4\text{N}][\text{Ia}]$

(a) Bond Distances (\AA)			
Tl-Fe	2.568 (2)	Tl-N1	2.61 (1)
N1-C1A	1.31 (1)	N1-C1E	1.34 (1)
C1A-C1B	1.41 (2)	C1B-C1C	1.43 (2)
C1C-C1D	1.36 (2)	C1D-C1E	1.38 (2)
C1A-C1AA	1.52 (2)		
(b) Bond Angles (deg)			
Fe-Tl-Fe1A	152.89 (8)	N1-Tl-N1A	62.7 (4)
Fe1-Tl-N1	97.3 (2)	Fe1-Tl-N1A	105.9 (2)
C1-Fe1-Tl	85.2 (4)	C2-Fe1-Tl	85.5 (4)
C3-Fe1-Tl	83.9 (4)	C4-Fe1-Tl	179.2 (5)

flections that should be equivalent in this crystal system showed that the Laue group was only mmm , as is also evident in the F_o/F_c listing.

Attempts were made to structurally characterize the ethylenediamine adduct. Crystals were grown by dissolving 0.15 g (0.11 mmol) of $[\text{Et}_4\text{N}]_2[\text{Ti}_2\text{Fe}_4(\text{CO})_{16}]$ in 10 mL of CH_2Cl_2 . A few drops of ethylenediamine were added, followed by addition of anhydrous diethyl ether and cooling. A golden crystalline material was obtained, which was then separated by filtration. The filtrate gave orange crystals upon standing at room temperature. Several crystals were examined for suitability for single-crystal X-ray diffraction, but all were twinned. Crystals grown from concentrated MeOH solutions were also unsuitable.

Positional parameters for $[\text{Et}_4\text{N}][\text{Ia}]$, $[\text{Et}_4\text{N}][\text{Ib}]$, $[\text{Et}_4\text{N}][\text{Ic}]$, and $[\text{Et}_4\text{N}][\text{Id}]$ are provided in Tables II-V, and selected bond distances and angles are shown in Tables VI-IX. Additional structural data are

Table VII. Selected Bond Distances and Angles for $[\text{Et}_4\text{N}][\text{Ib}]$

(a) Bond Distances (\AA)			
Tl-Fe1	2.573 (3)	Tl-N1	2.58 (1)
N1-C11	1.33 (2)	N1-C15	1.34 (2)
C11-C12	1.45 (2)	C12-C13	1.34 (3)
C13-C14	1.42 (3)	C14-C15	1.44 (2)
C15-C15A	1.43 (3)	C16-C16A	1.37 (6)
(b) Bond Angles (deg)			
Fe1-Tl-Fe1A	156.8 (1)	N1-Tl-N1	63.2 (5)
Fe1-Tl-N1	95.7 (3)	Fe1-Tl-N1A	104.1 (3)
C1-Fe1-Tl	85.3 (6)	C2-Fe1-Tl	86.6 (7)
C3-Fe1-Tl	83.9 (5)	C4-Fe1-Tl	175.6 (6)

Table VIII. Selected Bond Distances and Angles for $[\text{Et}_4\text{N}][\text{Ic}]$

(a) Bond Distances (\AA)			
Tl1-Fe1	2.610 (4)	Tl1-Fe2	2.612 (4)
Tl1-N1	2.65 (2)	Tl1-N2	2.66 (2)
N1-C1A	1.51 (3)	N1-C1B	1.54 (3)
N1-C3B	1.56 (3)	N2-C2A	1.48 (3)
N2-C2B	1.48 (3)	N2-C3A	1.44 (3)
C3A-C3B	1.49 (3)		
(b) Bond Angles (deg)			
Fe1-Tl1-Fe2	136.7 (1)	N1-Tl1-N2	72.7 (6)
Fe1-Tl1-N1	108.4 (5)	Fe1-Tl1-N2	106.7 (5)
Fe2-Tl1-N1	106.7 (5)	Fe2-Tl1-N2	107.3 (5)
C11-Fe1-Tl1	82.2 (8)	C21-Fe2-Tl1	79 (1)
C12-Fe1-Tl1	93 (1)	C22-Fe2-Tl1	82.6 (8)
C13-Fe1-Tl1	81.2 (8)	C23-Fe2-Tl1	95.3 (9)
C14-Fe1-Tl1	171 (1)	C24-Fe2-Tl1	169 (1)

Table IX. Selected Bond Distances and Angles for $[\text{Et}_4\text{N}][\text{Id}]$

(a) Bond Distances (\AA)			
Tl1-Fe1	2.605 (2)	Tl1-Fe2	2.615 (2)
Tl1-N1	2.61 (1)	Tl1-N2	2.55 (1)
Tl1...N3	3.02 (2)	N1-C1	1.46 (2)
N2-C2	1.43 (2)	N2-C3	1.43 (2)
N3-C4	1.28 (3)	C1-C2	1.47 (3)
C3-C4	1.50 (3)		
(b) Bond Angles (deg)			
Fe1-Tl1-Fe2	143.75 (7)	N1-Tl1-N2	67.9 (4)
N2-Tl1-N3	59.7 (5)	N1-Tl1-N3	127.6 (6)
Fe1-Tl1-N1	100.0 (3)	Fe1-Tl1-N2	108.8 (3)
Fe1-Tl1-N3	96.2 (4)	Fe2-Tl1-N1	100.1 (3)
Fe2-Tl1-N2	106.6 (3)	Fe2-Tl1-N3	95.1 (4)
C11-Fe1-Tl1	83.3 (5)	C21-Fe2-Tl1	86.7 (5)
C12-Fe1-Tl1	82.8 (5)	C22-Fe2-Tl1	82.7 (5)
C13-Fe1-Tl1	89.7 (5)	C23-Fe2-Tl1	82.4 (5)
C14-Fe1-Tl1	174.0 (6)	C24-Fe2-Tl1	175.2 (6)

available (see supplementary materials paragraph).

Results

Syntheses of $[\text{Et}_4\text{N}][\text{Ia}]$, $[\text{Et}_4\text{N}][\text{Ib}]$, $[\text{Et}_4\text{N}][\text{Ic}]$, $[\text{Et}_4\text{N}][\text{Id}]$, and $[\text{Et}_4\text{N}][\text{Ie}]$. Addition of a variety of Lewis bases to $[\text{Et}_4\text{N}]_2[\text{Ti}_2\text{Fe}_4(\text{CO})_{16}]$ in solution resulted in the formation of adducts with a Lewis base:Tl ratio of 1:1. The crystalline products varied in color from yellow to orange for $[\text{Et}_4\text{N}][\text{Ia}]$, $[\text{Et}_4\text{N}][\text{Ib}]$, $[\text{Et}_4\text{N}][\text{Ie}]$, and $[\text{Et}_4\text{N}][\text{Id}]$ to dark red for $[\text{Et}_4\text{N}][\text{Ic}]$. The adducts were soluble in CH_2Cl_2 , THF, and most polar organic solvents, although some decomposition was noted for $[\text{Et}_4\text{N}][\text{Ie}]$ in CH_2Cl_2 and $[\text{Et}_4\text{N}][\text{Id}]$ in CH_2Cl_2 and MeOH. Solution and solid-state IR spectra of all compounds except $[\text{Et}_4\text{N}][\text{Ic}]$ reveal a shifting of the strongest ν_{CO} bands to lower energy in comparison to those for the starting compound $[\text{Et}_4\text{N}]_2[\text{Ti}_2\text{Fe}_4(\text{CO})_{16}]$ (see Table X), which is consistent with an increased electron density at thallium and iron and concomitant reduction of C-O bond order. ^1H NMR spectra show a downfield shift of the Lewis base protons upon complexation versus the free ligand (see Table XI), indicating a decrease in proton shielding as electron density is transferred from the Lewis base to the thallium.

Structures of $[\text{Et}_4\text{N}][\text{Ia}]$, $[\text{Et}_4\text{N}][\text{Ib}]$, $[\text{Et}_4\text{N}][\text{Ic}]$, $[\text{Et}_4\text{N}][\text{Id}]$, and $[\text{Et}_4\text{N}][\text{Ie}]$. X-ray structural analyses of $[\text{Et}_4\text{N}][\text{Ia}]$, $[\text{Et}_4\text{N}][\text{Ib}]$, $[\text{Et}_4\text{N}][\text{Ic}]$, and $[\text{Et}_4\text{N}][\text{Id}]$ show asymmetric units consisting of ordered $[\text{Et}_4\text{N}]^+$ cations and $[(\text{L})\text{TiFe}_2(\text{CO})_8]^-$ anions (L = bpy,

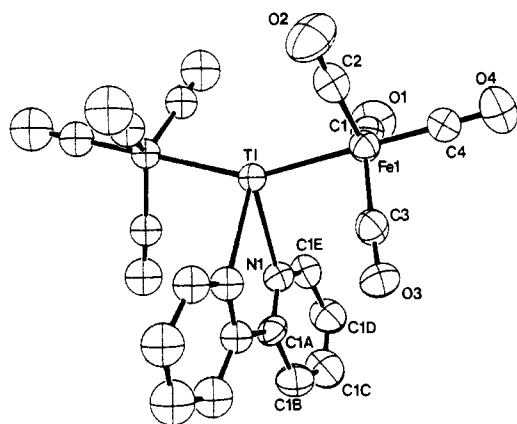
Table X. Infrared Data for Adducts and Free Ligands

compd	phase	ν_{CO} , cm^{-1}
$[\text{Et}_4\text{N}]_2[\text{Ti}_2\text{Fe}_4(\text{CO})_{16}]$	Nujol mull	1988 (s), 1920 (s), 1895 (s), 1873 (s)
	MeOH	1980 (s), 1910 (s)
$[\text{Et}_4\text{N}][(\text{bpy})\text{TiFe}_2(\text{CO})_8]$	MeOH	2008 (sh), 2000 (sh), 1980 (s), 1910 (s)
	Nujol mull	2000 (m), 1963 (s), 1913 (s), 1860 (s, br)
$[\text{Et}_4\text{N}][(\text{phen})\text{TiFe}_2(\text{CO})_8]$	CH_2Cl_2	2000 (m), 1985 (s), 1965 (s), 1889 (s, br)
	Nujol mull	2000 (m), 1964 (s), 1911 (s), 1860 (s, br)
$[\text{Et}_4\text{N}][(\text{en})\text{TiFe}_2(\text{CO})_8]$	CH_2Cl_2	2000 (m), 1984 (s), 1964 (s), 1889 (s, br)
	Nujol mull	1990 (m), 1971 (s), 1955 (s), 1855 (s, br)
$[\text{Et}_4\text{N}][(\text{TMEDA})\text{TiFe}_2(\text{CO})_8]$	MeOH	1980 (s), 1910 (s)
	Nujol mull	1994 (s), 1969 (s, sh), 1957 (s), 1907 (s), 1868 (s, br)
$[\text{Et}_4\text{N}][(\text{dien})\text{TiFe}_2(\text{CO})_8]$	acetone	1997 (m), 1982 (s), 1964 (s), 1888 (s, br)
	Nujol mull	1988 (m), 1951 (sh), 1810 (s, br)

Table XI. ^1H NMR Data

compd	chem shift, ppm vs $\text{MeCN-}d_3^a$
bpy	7.37 (t), 7.87 (t), 8.42 (d), 8.65 (d)
$[\text{Et}_4\text{N}][(\text{bpy})\text{TiFe}_2(\text{CO})_8]$	7.40 (t), 7.90 (t), 8.37 (d), 8.66 (d)
phen	7.70 (q), 7.90 (s), 8.38 (d), 9.12 (d)
$[\text{Et}_4\text{N}][(\text{phen})\text{TiFe}_2(\text{CO})_8]$	7.86 (q), 8.02 (s), 8.56 (d), 9.17 (d)
en ^b	1.16 (s), 2.60 (s)
$[\text{Et}_4\text{N}][(\text{en})\text{TiFe}_2(\text{CO})_8]^b$	1.60 (s), 2.89 (s)
TMEDA	2.15 (s), 2.30 (s)
$[\text{Et}_4\text{N}][(\text{TMEDA})\text{TiFe}_2(\text{CO})_8]$	2.23 (s), 2.40 (s)
dien ^b	1.27 (s), 2.67 (s)
$[\text{Et}_4\text{N}][(\text{dien})\text{TiFe}_2(\text{CO})_8]^b$	1.64 (s, br), 2.97 (s, br)

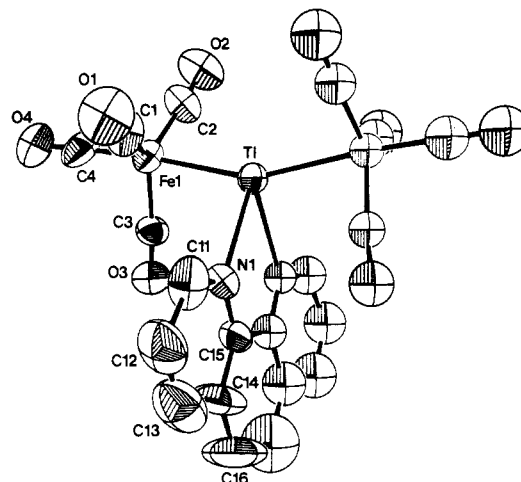
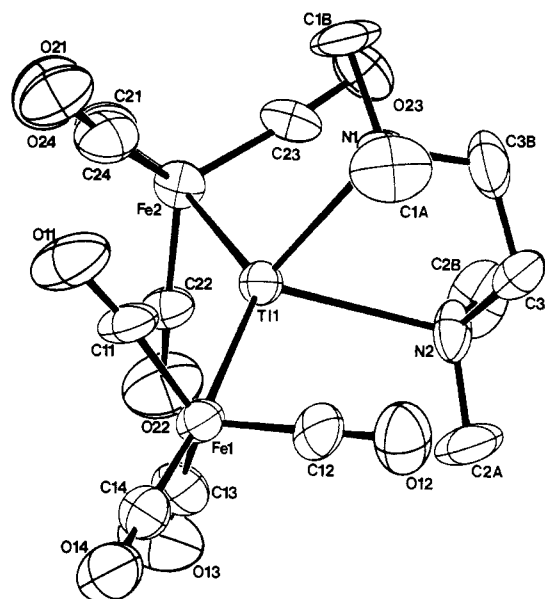
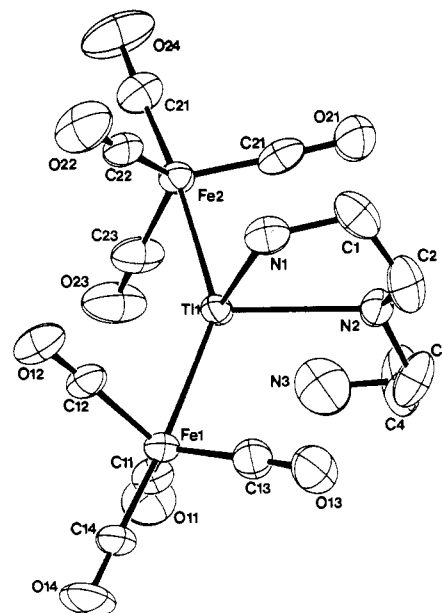
^aChemical shifts not given for $[\text{Et}_4\text{N}]^+$. ^bChemical shifts for these compounds are reported as ppm vs CD_2Cl_2 .

**Figure 1.** ORTEP diagram and atom-labeling scheme for the anion $[\text{Ia}]^-$, $[(\text{bpy})\text{TiFe}_2(\text{CO})_8]^-$.

phen, TMEDA, dien) in a 1:1 ratio. ORTEP diagrams of the anions are given in Figures 1–4. The anions each exhibit a central four-coordinate thallium of highly distorted tetrahedral geometry. The thalliums are each coordinated to two trigonal-bipyramidal $\text{Fe}(\text{CO})_4$ groups, with the thalliums occupying axial sites, and to two nitrogens of the donor ligand. Little deviation from linearity is observed for the carbonyls with $\angle\text{Fe-C-O}$ values ranging from $172(2)$ to $180(1)^\circ$. Almost all of the equatorial carbonyls show some bending toward the thallium atoms.

Discussion

To date, only a limited number of thallium-containing carbonyls are known. Examples include the thallium-cobalt series $\text{Tl}[\text{Co}(\text{CO})_4]_2$,^{6,7} $\text{Tl}[\text{Co}(\text{CO})_4]_3$,^{6,8} and $[\text{Tl}[\text{Co}(\text{CO})_4]_4]^-$,⁹

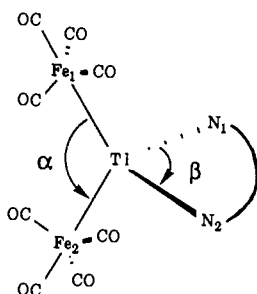
**Figure 2.** ORTEP diagram and atom-labeling scheme for the anion $[\text{Ib}]^-$, $[(\text{phen})\text{TiFe}_2(\text{CO})_8]^-$.**Figure 3.** ORTEP diagram and atom-labeling scheme for the anion $[\text{Ic}]^-$, $[(\text{TMEDA})\text{TiFe}_2(\text{CO})_8]^-$.**Figure 4.** ORTEP diagram and atom-labeling scheme for the anion $[\text{Id}]^-$, $[(\text{dien})\text{TiFe}_2(\text{CO})_8]^-$.

(6) Hieber, W.; Teller, U. *Z. Anorg. Allg. Chem.* **1942**, *249*, 43.

Table XII. Comparison of Core Geometry Parameters for $[\text{Et}_4\text{N}][\text{Ia}]$, $[\text{Et}_4\text{N}][\text{Ib}]$, $[\text{Et}_4\text{N}][\text{Ic}]$, and $[\text{Et}_4\text{N}][\text{Id}]^a$

	$[\text{Et}_4\text{N}][\text{Ia}]$	$[\text{Et}_4\text{N}][\text{Ib}]$	$[\text{Et}_4\text{N}][\text{Ic}]$	$[\text{Et}_4\text{N}][\text{Id}]$
$d_{\text{Ti-Fe}}$, Å	2.568 (2)	2.573 (3)	2.610 (4)	2.605 (2)
			2.612 (4)	2.615 (2)
$d_{\text{Ti-N}}$, Å	2.61 (1)	2.58 (1)	2.65 (2)	2.61 (1)
			2.66 (2)	2.55 (1)
α , deg	152.89 (8)	156.8 (1)	136.7 (1)	143.75 (7)
β , deg	62.7 (4)	63.2 (5)	72.7 (6)	67.9 (4)

^a Parameters are defined by the following diagram:



and $\text{Ti}[\text{Mn}(\text{CO})_5]_3$,¹⁰ $\text{Ti}[(\text{C}_5\text{H}_4\text{CHPh}_2)\text{Cr}(\text{CO})_3]_3$,¹¹ $\text{Ti}[\text{Mo}(\text{CO})_3\text{Cp}]_2$ (Cp = cyclopentadienyl),^{12,13} and $\text{Ti}[\text{M}(\text{CO})_3\text{Cp}]$ (M = Cr, Mo, W).¹⁴ Several of these compounds display interesting properties. The three-coordinate thallium-manganese carbonyl $\text{Ti}[\text{Mn}(\text{CO})_5]_3$ is thermochromic, changing from dark red to pale red upon cooling.¹⁰ Also $\text{Ti}[\text{Mn}(\text{CO})_5]_3$ and a number of other thallium-metal carbonyls undergo light-induced disproportionation.¹⁴ The crystals of $\text{Ti}[\text{Mo}(\text{CO})_3\text{Cp}]_3$ exhibit a red/green dichroism.^{12,13} Until recently only two thallium-metal carbonyl compounds, $\text{Ti}[\text{Co}(\text{CO})_4]_7$ and $\text{Ti}[\text{Mo}(\text{CO})_3\text{Cp}]_3$,¹³ had been structurally characterized.

The new Tl-Fe carbonyl clusters, $[\text{Et}_4\text{N}]_2[\text{Ti}_2\text{Fe}_4(\text{CO})_{16}]$,^{1a} $[\text{PPN}]_2[\text{Ti}_2\text{Fe}_6(\text{CO})_{24}]$,¹⁵ $[\text{Et}_4\text{N}]_4[\text{Ti}_4\text{Fe}_8(\text{CO})_{30}]$,^{1a} and $[\text{Et}_4\text{N}]_6[\text{Ti}_6\text{Fe}_{10}(\text{CO})_{36}]$ ^{1a,2} have been structurally characterized and can be viewed as dimers. For $[\text{Et}_4\text{N}][\text{I}]$ the structural parameters and its IR and ¹³C NMR spectra imply the existence of the monomer in solution.^{1a} The loss in electron density at thallium when in the monomer form may be lessened through solvent donation, although no solvent-coordinated compound has yet been isolated. The fact that the Lewis base adducts can be produced, as described herein, supports the idea that $[\text{Et}_4\text{N}]_2[\text{Ti}_2\text{Fe}_4(\text{CO})_{16}]$ is a monomer in solution, although not conclusively, as Lewis bases are known to cleave oligomers.¹⁶

The thallium atom in each adduct exhibits a highly distorted tetrahedral geometry. Comparisons are made in Table XII for compounds $[\text{Et}_4\text{N}][\text{Ia}]$ – $[\text{Et}_4\text{N}][\text{Id}]$. The Fe–Tl–Fe angles are 136.7 (1) and 143.75 (7)° and the N–Tl–N angles are 72.7 (6) and 67.9 (4)° for $[\text{Et}_4\text{N}][\text{Ic}]$ and $[\text{Et}_4\text{N}][\text{Id}]$, respectively. In comparison, the Fe–Tl–Fe angles in $[\text{Et}_4\text{N}][\text{Ia}]$ and $[\text{Et}_4\text{N}][\text{Ib}]$ are 152.89 (8) and 156.8 (1)° and the N–Tl–N angles are 62.7 (4) and 63.2 (5)°, respectively. The smaller Fe–Tl–Fe angles in $[\text{Et}_4\text{N}][\text{Ic}]$ and $[\text{Et}_4\text{N}][\text{Id}]$ are most likely due to steric effects

caused by interactions of the bulkier, less rigid Lewis base ligands with the $\text{Fe}(\text{CO})_4$ groups. One might also argue that in $[\text{Et}_4\text{N}][\text{Ia}]$ and $[\text{Et}_4\text{N}][\text{Ib}]$ the sp^2 coordination of the nitrogens of the bipyridine and phenanthroline ligands, when compared to the sp^3 coordination of the nitrogens of the tetramethylethylenediamine and diethylenetriamine ligands, creates greater s character in the Tl–Fe bonds leading to larger Fe–Tl–Fe bond angles.

In almost all cases equatorial CO ligands (see Tables VI–IX) are tilted toward the thallium. This bending toward the main-group atom, here and in related compounds, is common and is normally attributed to the slight ionicity of the heterobimetallic bond. Compounds that exhibit this type of carbonyl bending include $[\text{CdFe}(\text{CO})_4]_4 \cdot 2\text{C}_3\text{H}_6\text{O}$,¹⁵ $[(\text{bpy})\text{CdFe}(\text{CO})_4]_3 \cdot 3/4\text{C}_6\text{H}_5\text{Cl}_3$,¹⁶ $[\text{Na}(\text{THF})_2]_2^{2+}[\text{M}(\text{Fe}(\text{CO})_4)_2]^{2-}$ (M = Zn, Cd, Hg),¹⁷ $[\text{Et}_4\text{N}]_2[\text{Fe}_3(\text{CO})_9(\mu_3\text{-CO})(\mu_3\text{-GeFe}(\text{CO})_4)]$,¹⁸ $[\text{Et}_4\text{N}]_2[\text{Pb}(\text{Fe}(\text{CO})_4)_2(\text{Fe}_2(\text{CO})_8)]$,¹⁹ and $\text{Bi}[\text{Mn}(\text{CO})_5]_3$,²⁰ as well as the thallium-iron carbonyls $[\text{Et}_4\text{N}]_2[\text{Ti}_2\text{Fe}_4(\text{CO})_{16}]$, $[\text{Et}_4\text{N}]_4[\text{Ti}_4\text{Fe}_8(\text{CO})_{30}]$, and $[\text{Et}_4\text{N}]_6[\text{Ti}_6\text{Fe}_{10}(\text{CO})_{36}]$.^{1a}

In $[\text{Et}_4\text{N}][\text{Id}]$ the noncoordinated diethylenetriamine nitrogen is oriented toward the thallium atom (Tl–N3 = 3.02 (2) Å), instead of in a more sterically favored position. This fact may indicate a weak bonding interaction between the nitrogen and the thallium. The close proximity of the nitrogen to thallium and the broadening of the peaks observed in the ¹H NMR spectrum suggest that an equilibrium between coordination and noncoordination may be occurring in solution.

Formally, the thallium atom can be considered as a 1- ion donating all of its valence electrons to neutral irons. Since each thallium atom also obtains two pairs of electrons from a bidentate Lewis base, each thallium is surrounded by eight electrons and obtains a filled octet. Thus, the thallium adducts should be good representations of single Tl–Fe (terminal) bonds. The Tl–Fe bonds of $[\text{Et}_4\text{N}][\text{Ia}]$ and $[\text{Et}_4\text{N}][\text{Ib}]$ are 2.568 (2) and 2.573 (3) Å, respectively, and the Tl–Fe distances average 2.611 (4) and 2.610 (2) Å for $[\text{Et}_4\text{N}][\text{Ic}]$ and $[\text{Et}_4\text{N}][\text{Id}]$, respectively. The small differences in the Tl–Fe bond lengths are probably due to steric interactions of the different ligands with the $\text{Fe}(\text{CO})_4$ groups. In comparing the Tl–Fe bonds of the adducts to the terminal Tl–Fe bonds in $[\text{Et}_4\text{N}]_2[\text{Ti}_2\text{Fe}_4(\text{CO})_{16}]$ (Tl–Fe = 2.552 (5) Å), $[\text{Et}_4\text{N}]_4[\text{Ti}_4\text{Fe}_8(\text{CO})_{30}]$ (Tl–Fe = 2.530 (7) Å), and $[\text{Et}_4\text{N}]_6[\text{Ti}_6\text{Fe}_{10}(\text{CO})_{36}]$ (Tl–Fe = 2.561 (4) and 2.530 (7) Å),^{1a} we note that the adduct single-bond Tl–Fe lengths are only slightly longer than any of the Tl–Fe terminal bonds in these cluster compounds. The substantial shortening expected for a multiple-bond interaction is not observed, indicating that steric and electrostatic effects may be more important in determining the bonding parameters of these compounds.

Acknowledgment. The National Science Foundation (Grant CHE-8421217) and the Robert A. Welch Foundation are gratefully acknowledged for support of this work.

Registry No. $[\text{Et}_4\text{N}][\text{Ia}]$, 119681-21-9; $[\text{Et}_4\text{N}][\text{Ib}]$, 119681-23-1; $[\text{Et}_4\text{N}][\text{Ic}]$, 119681-25-3; $[\text{Et}_4\text{N}][\text{Id}]$, 119681-27-5; $[\text{Et}_4\text{N}][\text{Ie}]$, 119681-29-7; $[\text{Et}_4\text{N}]_2[\text{Ti}_2\text{Fe}_4(\text{CO})_{16}]$, 113218-98-7; $[\text{Et}_4\text{N}][\text{TiFe}_2(\text{CO})_8]$, 104337-74-8; Fe, 7439-89-6; Tl, 7440-28-0.

Supplementary Material Available: Listings of complete crystallographic data collection parameters, anisotropic thermal parameters, and complete bond distances and angles (18 pages); tables of calculated and observed structure factors for $[\text{Et}_4\text{N}][\text{Ia}]$, $[\text{Et}_4\text{N}][\text{Ib}]$, $[\text{Et}_4\text{N}][\text{Ic}]$, and $[\text{Et}_4\text{N}][\text{Id}]$ (60 pages). Ordering information is given on any current masthead page.

- (7) Schussler, D. P.; Robinson, W. R.; Edgell, W. F. *Inorg. Chem.* **1974**, *13*, 153.
- (8) Patmore, D. J.; Graham, W. A. G. *Inorg. Chem.* **1966**, *5*, 1586.
- (9) Robinson, W. R.; Schussler, D. P. *J. Organomet. Chem.* **1971**, *30*, C5.
- (10) Hsieh, A. T. T.; Mays, M. J. *J. Organomet. Chem.* **1970**, *22*, 29.
- (11) Cooper, R. L.; Fischer, E. O.; Semmlinger, W. *J. Organomet. Chem.* **1967**, *9*, 333.
- (12) King, R. B. *Inorg. Chem.* **1970**, *9*, 1936.
- (13) Rajaram, J.; Ibers, J. A. *Inorg. Chem.* **1973**, *12*, 1313.
- (14) Burlitch, J. M.; Theyson, T. W. *J. Chem. Soc., Dalton Trans.* **1974**, 828.
- (15) Cassidy, J. M.; Whitmire, K. H. See preceding paper in this issue.
- (16) (a) Ernst, R. D.; Marks, T. J.; Ibers, J. A. *J. Am. Chem. Soc.* **1977**, *99*, 2090. (b) Ernst, R. D.; Marks, T. J.; Ibers, J. A. *J. Am. Chem. Soc.* **1977**, *99*, 2098.

- (17) Sosinsky, B. A.; Shong, R. G.; Fitzgerald, B. J.; Norem, N.; O'Rourke, C. *Inorg. Chem.* **1983**, *22*, 3124.
- (18) Whitmire, K. H.; Lagrone, C. B.; Churchill, M. R.; Fettingter, J. C.; Robinson, B. H. *Inorg. Chem.* **1987**, *26*, 3491.
- (19) Lagrone, C. B.; Whitmire, K. H.; Churchill, M. R.; Fettingter, J. C. *Inorg. Chem.* **1986**, *25*, 2080.
- (20) Wallis, J. M.; Müller, G.; Schmidbaur, H. *Inorg. Chem.* **1987**, *26*, 458.